Dynamic Focusing Microlens Array using a Liquid Crystalline Polymer and a Liquid Crystal

Yoonseuk Choi*[a] , Kwang-Ho Lee[b], Hak-Rin Kim[a], and Jae-Hoon Kim[a,b]
[a]Research Institute of Information Display, Hanyang University,
17 Haengdang-Dong, Seongdong-Gu, Seoul 133-791, Korea;
[b]Department of Electronics and Computer Engineering, Hanyang University,
17 Haengdang-Dong, Seongdong-Gu, Seoul 133-791, Korea

ABSTRACT

An active microlens device is demonstrated by using a stacked layer structure of UV curable polymer, liquid crystalline polymer (LCP) and a liquid crystal (LC). The incident linearly polarized light is focused after passing through the combined refractive type microlens array system of UV curable polymer and LCP. Because used LCP shows highly birefringent macroscopic property from the well-ordered molecular structure, the additional polarization state control layer was inserted to modulate the dynamic focusing characteristics of the device. From the additional twisted LC layer's electro-optic response, we obtained good focal switching characteristics of microlens array with a small operation voltage application. This enhanced dynamic focusing characteristic of device was originated from the separate operation of polymer lens structure's beam focusing and twisted LC layer's polarization control ability. The measured focal length was well matched to the calculated one. This proposed LC microlens array is expected to play a critical role in the various real photonic components such as highly reliable optical switch, beam modulator and key device for 3-D imaging system.

Keywords: microlens array, liquid crystal, liquid crystalline polymer, dynamic focusing, twisted LC structure, UV curable polymer

1. INTRODUCTION

1.1 Current LC Microlenses

With the technological progress in optics, the need for microlens has been increased for its diverse electro-optical applications such as optical interconnections, photonic devices, integrated optical components and optical communication system. Particularly, in the field of microlens development, the most viable approach is a liquid crystal (LC) based microlens which can easily provide dynamic focusing properties of the device with an electric field engagement.

Until now, various types of the LC based device configurations have been investigated to realize diverse dynamic properties of microlens array, for example, adopting designed electrode pattern, modulating spatial dielectric property and LC director controlling by polymer stabilized structure [1-14]. Many of existing LC microlens structure, they used gradient refractive-index (GRIN) profile of LCs produced by a specially designed electric field pattern or a surface relief structure to obtain and control the dynamic focusing properties of the device. However, in most these efforts, some limits were pointed such as limiting focus tunability, slow switching speed, complex fabrication process, instable device operation property and high driving voltage. Especially, the dynamic characteristics of focus switching were not acceptable for the real photonic applications due to the intrinsic limits of GRIN effect based focusing scheme like the reverse tilt of LCs' reorientation during electrical driving.

1.2 Motivation of This Work

In this paper, we demonstrate a novel type of electronically switchable microlens array which is composed of a stacked layer structure of UV curable polymer, liquid crystalline polymer (LCP) and a LC. In our configuration, the incident

Optoelectronic Materials and Devices, edited by Yong Hee Lee, Fumio Koyama, Yi Luo,
Proc. of SPIE Vol. 6352, 63521H, (2006) · 0277-786X/06/$15 · doi: 10.1117/12.691799

linearly polarized light is focused after passing through the lens-shaped boundary between UV curable polymer and LCP layer due to the light refraction effect from different refractive indexes of surrounding materials. The surface relief structure for microlens array can be simply obtained by the spin-coating process and UV irradiation through an appropriate photomask. As the LCP shows birefringent optical characteristics, the focusing scheme of our microlens can be easily controlled by choosing the incident polarization state of light. Therefore, the additional twisted nematic (TN) LC structure was inserted on the polymer lens layer in our configuration to control the incident light polarization. As the result, the dynamic focusing characteristics of device was obtained from the separate operation of double polymer layer's beam focusing and LC layer's polarization control ability. By engaging an external voltage to this LC microlens array, we can obtain a focal switching characteristic of the device within a simple fabrication process. Moreover because the rubbed LC alignment induced well-ordering LCP layer can promote a uniform planar alignment of LC molecules at the interface, we can easily construct the polarization controlling LC layer (in our study, twisted structure) on the polymer surface without any specific additional treatment.

2. DYNAMIC LC MICROLENS BASED ON LCP

2.1 Device Configuration

Suggested new LC microlens configuration can be divided into two sub-parts by the function for driving. In first, a microlens array structure was prepared by a concave lens-shaped surface relief of UV curable polymer and an additionally filled LCP layer to achieve a refractive type convex lens operation. Because LCP has a birefringent nature similar to the conventional nematic LCs, we should generate the ordered LCP structure to promote the refractive index difference between LCP and UV curable polymer for lens operation. Therefore, homogeneous LC alignment layer was inserted to provoke the planar LCP alignment with unidirectional rubbing process. After casting and curing liquid-like LCP on this concave surface relief structure of UV curable polymer, we obtained a polymer microlens structure with a flat boundary which can act as a convex and a concave microlens simultaneously depending on the incident linear polarization state. In our configuration, we set the initially convex lens scheme for low-power driving by adding the twisted LC layer on the polymer microlens structure with a fixed input polarization direction. For TN LC structure homogeneous LC alignment layer was added and rubbed on the top indium-tin oxide (ITO) glass substrate, while nematic LCs are aligned to follow LCP ordering at the other interface. After engaging voltage, incident polarization doesn't change at all due to the vertically aligned LCs which results in beam diverging operation. This device configuration and operation state is simply illustrated in Fig. 1.

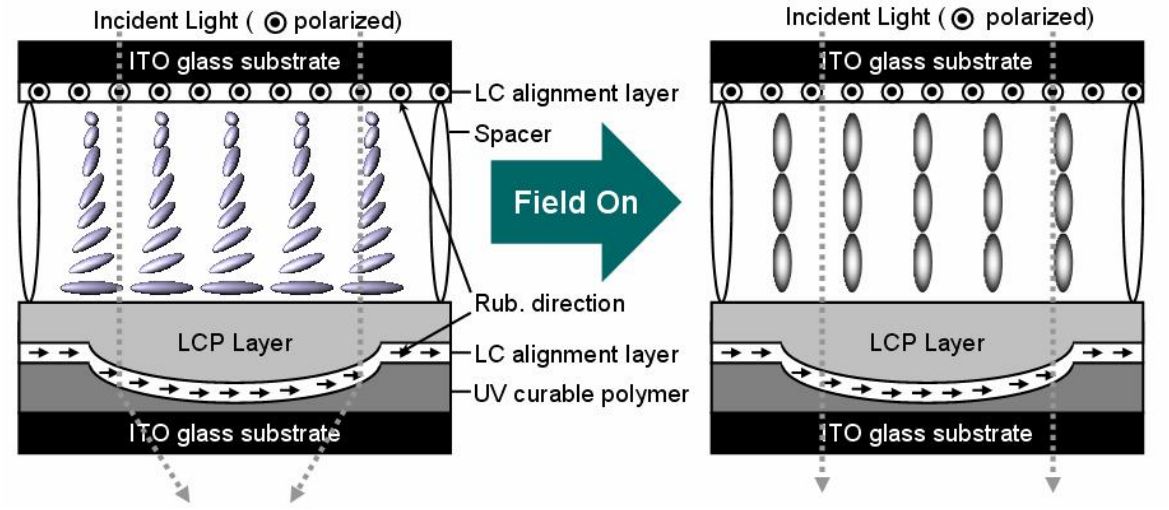

Fig. 1. Illustration of device configuration and its basic two operation state. The LCs was 90 degree twisted at initial state. Therefore incident linearly polarized light turned its polarization state as 90 degree after passing LC layer and focused due to the refraction effect at the polymer microlens. When the external field is on, because the incident polarization doesn't change after passing LC layer so that the incident light is defocused.

2.2 Operation Principle

Basic focusing mechanism of our microlens is using the refractive effect at the lens-shaped boundary of polymer structure from the effective refractive index difference of LCP and UV curable polymer. This double stacked polymer layer system can play as microlens of either convex or concave type with a flat surface boundary at the top depending on the incident polarization state. Control for incident polarization state of light was carried out at the TN LC layer which can simply manage the polarization state of light of various inputs by an applied voltage.

The focusing property of this polymer microlens array is sensitive to the incident light polarization state due to the birefringent feature of LCP. When the polarized direction (linear case) is parallel to the LCP's aligning direction (i.e. rubbing direction of bottom LC alignment layer), the incident light is focused because the beam experienced the extraordinary refractive index of LCP at the LCP layer which is bigger than the refractive index of UV curable polymer. Therefore, the polymer microlens gathered incident beam just like the refractive type convex lens as depicted in the left part of Fig. 1. The beam is de-focused (diverged) in the other case (i.e. field is on for producing homeotropic LC alignment and a perpendicularly polarized light is put to the LCP layer) because in this case the effective refractive index of LCP layer is an ordinary refractive index of LCP and this is smaller than that of UV curable polymer (see right illustration in Fig. 1). In our configuration, we set the device as a convex lens in initial because the beam focusing has much more application in practical applications. To control the focusing characteristics, a TN LC layer was promoted on the flat boundary polymer microlens structure as described before. Since the LCP has ability for aligning LCs due to the polymer chain ordering effect, no additional LC alignment layer was required in our research.

As the summary, without an applied voltage the incident linearly polarized light is focused by passing through the device when the incident polarization direction is parallel to the rubbing of top LC alignment layer as depicted in the Fig. 1. Otherwise, the LCs acts like an optically isotropic medium from the electric field induced homeotropic LC configuration. In this case, the de-focused state of device was obtained because the polarization direction of light emerging into the polymer microlens structure is perpendicular to the aligning direction of LCP. Since the polarization state of input beam can be continuously controlled from the extraordinary axis of the LCP to the ordinary axis with increasing an applied voltage in the TN LC structure, the focusing characteristic of device can be managed continuously with the applied voltages simply.

3. EXPERIMENT

3.1 Sample Fabrication

To examine the dynamic focusing characteristics of suggested microlens array, the experimental sample was fabricated by using two-sandwiched ITO glass substrates. Top substrate (see Fig. 1) was treated by a conventional homogeneous LC alignment layer with unidirectional rubbing process. For the bottom substrate, more complicated fabrication process was performed to obtain a polymer microlens structure consist of stacked system of UV curable polymer and LCP with flat surface. The detailed fabrication procedure was schematically explained in Fig. 2 (a). The thin UV curable polymer film was spin-coated on the cleaned bare ITO glass substrate in first (1^{st} and 2^{nd} cartoons in the Fig. 2). After that, we generate a relief profile of UV curable polymer by spatially selective UV irradiation through the designed amplitude photomask with controlling intensity and irradiation time. Then we can easily obtain the surface relief structure of UV curable polymer under high controllability as we desired due to the monomer diffusion effect before the polymerization (see 3^{rd} cartoon in Fig 2 (a)). In detail, the UV cured region of polymer was remained hard while the other region shaped concave lens structure gradually following the amplitude photomask as depicted in Fig. 2 (b). By using this method, we can easily obtain the opposite structure by adopting converse photomask [1-3,15,16]. Moreover, the curvature of microlens array can be varied by controlling a UV irradiation time and power. For next step, the conventional homogeneous LC alignment layer was spin-coated to make an ordered LCP layer. The LCP layer was spin-coated twice for obtaining flattened surface and cured with heat treatment of 60°C and UV (λ=365nm) irradiation process. As the result, a highly birefringent LCP film was produced on the concave surface relief with flat boundary conditions. This stacked polymer layer performs the beam focusing role in our LC microlens configuration as described in the previous section. The diameter of photomask (D) was 200μm and the distance between centers of circle (X,Y) was also the same in our experiment.

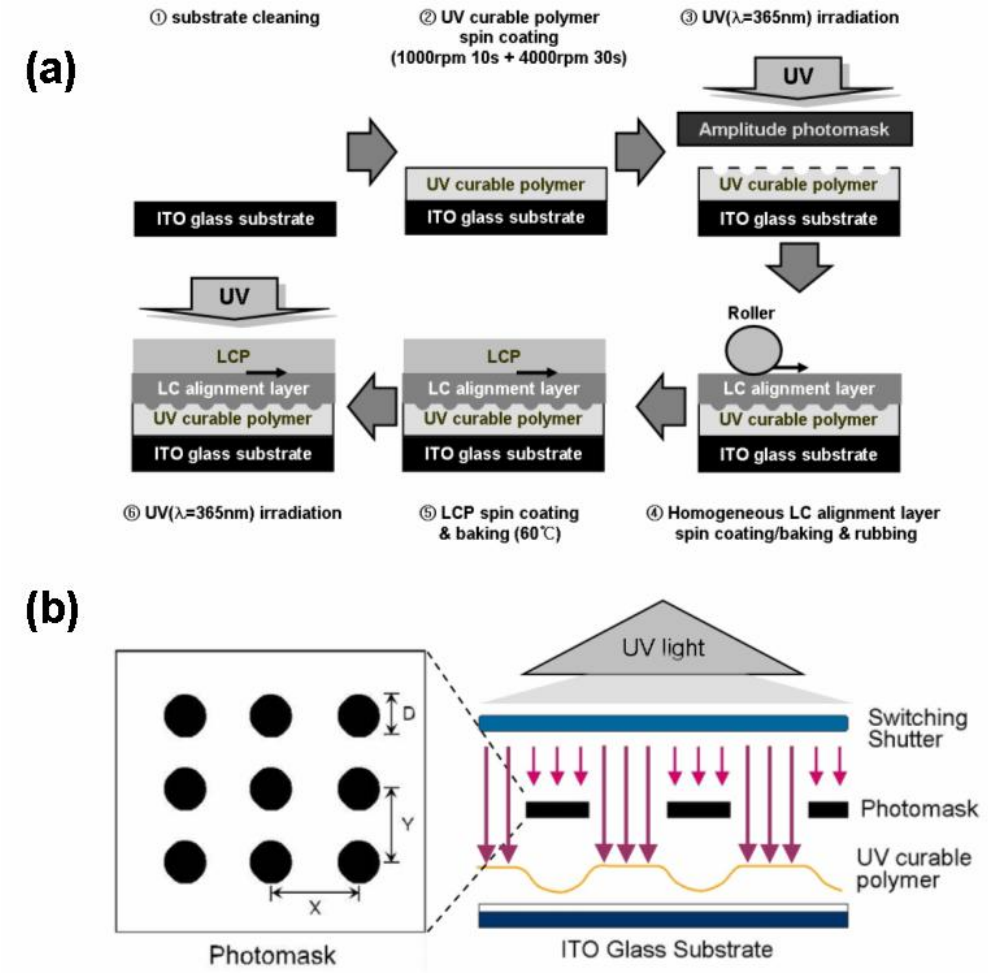

Fig. 2. Schematic illustrations for (a) Fabrication of bottom polymer microlens structure. From the bare ITO glass substrate, the concave lens-shaped surface relief structure of UV curable polymer was fabricated in first three steps. In next three steps, LCP layer was added with the treatment for making ordered LCP structure and stable construct with flat boundary condition. (b) Detailed illustration for fabricating surface relief construct of UV curable polymer with a single amplitude photomask and simple UV irradiation process briefly.

3.2 Material Characteristics

A commercial homogeneous LC aligning material RN-1199 of Nissan Chemical, a reactive mesogen (LCP) RMS03-001 of Merck, UV curable polymer NOA60 of Norland and a nematic LC MLC-6080 of Merck having a positive dielectric anisotropy were used in this experiment. The dielectric anisotropy of LC, the ordinary and extraordinary refractive indices of LCP at 590nm, the cured refractive index of the NOA60 were $\Delta\varepsilon = 7.2$, $n_{o\_LCP} = 1.529$, $n_{e\_LCP} = 1.684$ and $n_{polymer} = 1.56$, respectively. The cell gap for TN LC layer was maintained using glass spacers of 4μm thick and to achieve stable spacing through the whole sample, the LC was inserted by dropping method.

Microscopic textures of sample were acquired with a polarizing optical microscope (Nikon, ECLIPSE E600) under the crossed polarizers. All focal images were captured by using the simple He-Ne laser (633nm) setup [1-3], the CCD and a computer-controlled image grabbing system at the focal plane of LC microlens.

4. RESULTS AND DISCUSSION

4.1 LCP/UV Curable Polymer Microlens Structure

First, we examined the surface characteristics of polymer microlens structure with the scanning electron microscopic (SEM) images and the surface profile measurement. In Fig. 3, the photographs of surface morphology for UV curable polymer concave relief structure and LCP combined structure were represented in (a) and (c), respectively. We could easily confirm the concave microlens array structure in Fig. 3 (a) and flat surface LCP structure in Fig. 3 (b). Also, the surface profile for UV curable polymer and LCP were measured at the edge of structure as depicted in Fig. 3 (b) and (d), respectively. The diameter of each microlens array was about 200μm and the depth of relief was measured as 4μm. After making LCP layer on UV curable polymer relief structure, identically flat surface was observed as depicted in Fig. 3 (d) and in our measurement, LCP layer thickness and a whole polymer microlens thickness was about 2.3μm and 20μm, respectively. Therefore we can conclude that the double spin-coating of LCP layer was enough to achieve the flat boundary condition. Note that the thickness of polymer microlens structure can be reduced by optimizing spin-coating and UV irradiation conditions.

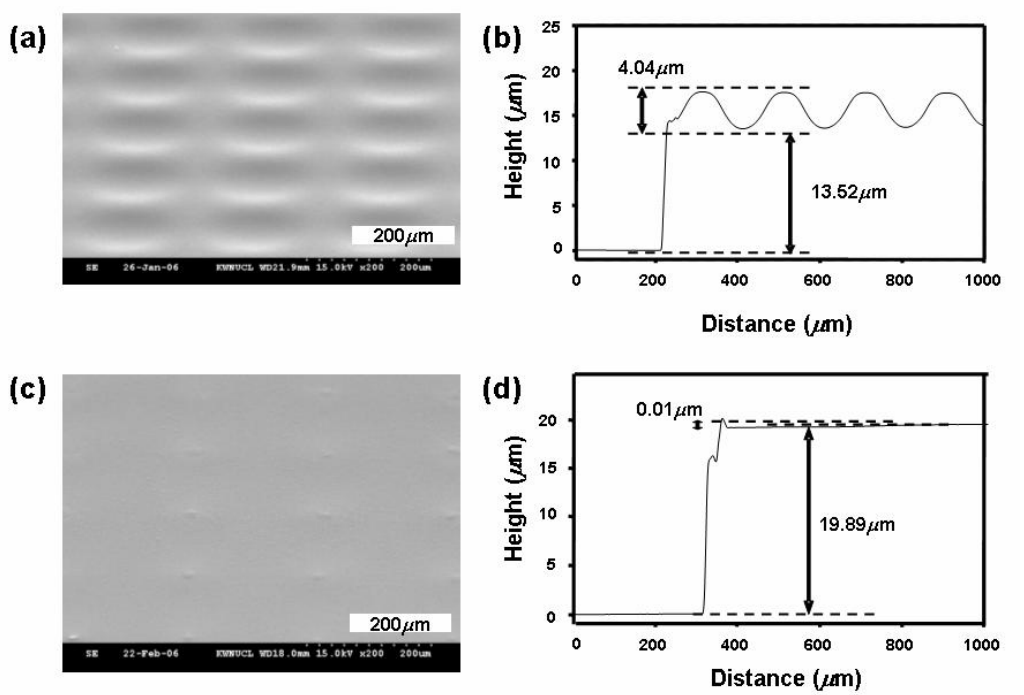

Fig. 3. Surface characteristics of UV curable polymer structure and LCP coated structure. (a) SEM photographs of concave microlens structure of UV curable polymer. (b) Surface profile measurement of UV curable polymer concave microlens array. (c) SEM photographs of polymer microlens structure after fabricating additional LCP layer. (d) Measured surface profile of stacked system for UV curable polymer and LCP. Note that in the SEM images, scale bars represent 200μm each.

From the microscopic texture observation under crossed polarizers, we confirmed that this polymer microlens array has an optically birefringent characteristic due to the additional LCP layer. Moreover, the uniform LCP alignment was also monitored by rotating the sample compared to external polarizers. When the rubbing direction of LC alignment layer was matched to the external crossed polarizer, complete dark image was observed while the other case shows light leakage from the birefringent feature. The microscopic photographs for LCP/UV curable polymer microlens structure was presented in Fig. 4.

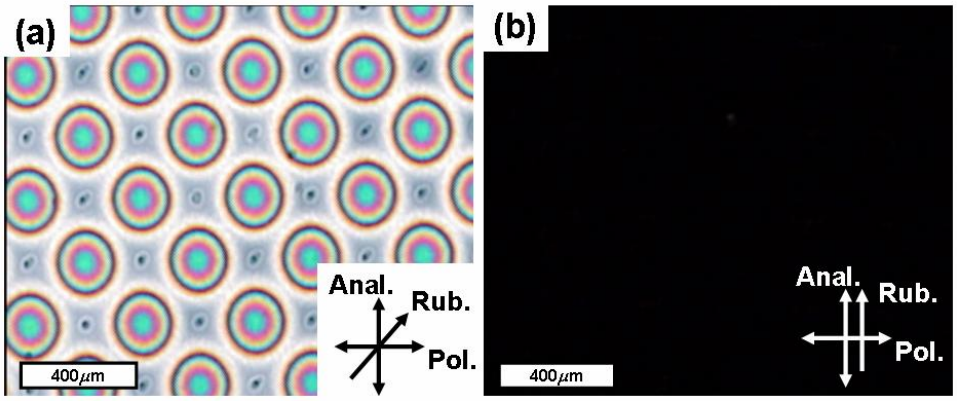

Fig. 4. Microscopic texture observation of fabricated polymer microlens array structure. (a) When the rubbing direction of LC alignment layer is 45 degree inclined to the external crossed polarizers, while (b) is parallel to the analyzer of monitoring system. Scale bar represents 400μm and all images were captured by CCD.

4.2 LC Texture Observation

In next, we examined the microscopic texture of device as shown in Fig. 5 for assuring the regular operation of additional TN LC mode. As observed in the figure, normally white TN LC structure was verified with the microscopic texture evidence as increasing the applied voltage. Complete dark image of the LC microlens (Fig. 5 (b)) with homeotropic LC alignment was obtained at the 10V application while light leakage was monitored at 0V application. This result is well matched to the conventional TN LC characteristic and the driving voltage is reasonable for practical application. The diameter of single LC microlens and the distance between lenses were 200μm each.

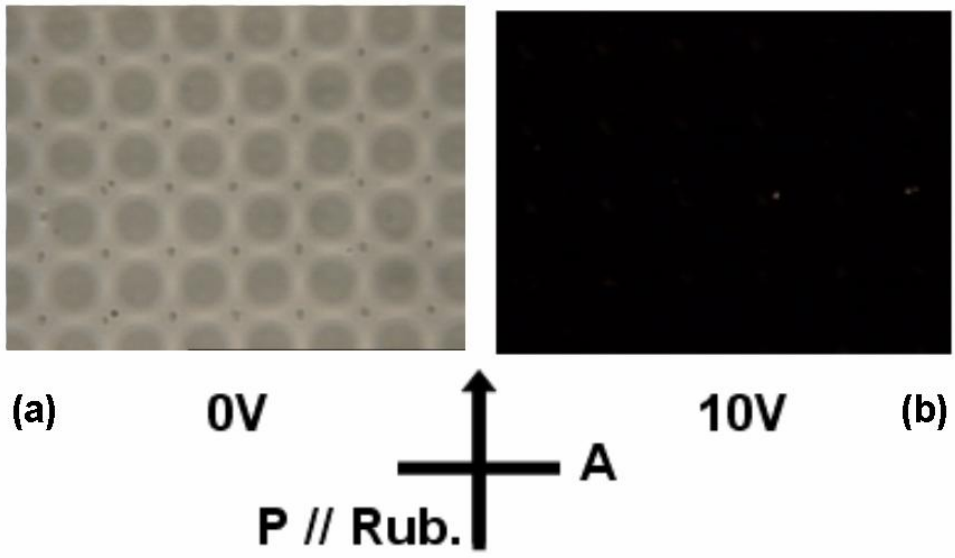

Fig. 5. Microscopic images of LC textures for our device under crossed polarizing microscope at various applied voltages of (a) 0V and (b) 10V.

4.3 Focusing Characteristics of Device

Figure 6 shows the focusing properties of our LC microlens under several applied voltages between 0V and 10V. Well focused beam array spots were observed at initial state of device as shown in Fig. 6 (a). This is weakened and blurred and finally almost disappeared as increasing applied voltage (5V, 6V, 10V). Remember that the polarization direction of incident beam is parallel to the rubbing direction of LC aligning material at top substrate in this experiment. Note that due to the threshold driving feature of TN LC mode, no particular focal characteristic change was monitored before the 5V application. This electric field controlled focus switching characteristics was originated from the incident polarization control ability of additional TN LC layer and birefringent aspect of polymer microlens structure as described before. In our experiment, 10V application was enough to switch the focus of LC microlens.

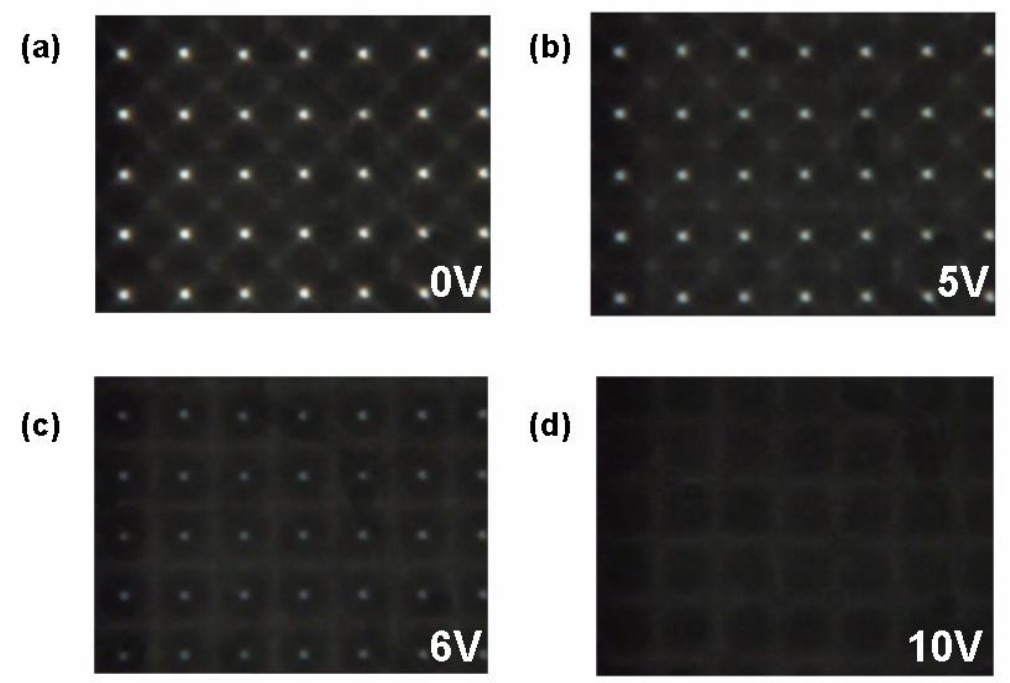

Fig. 6. Dynamic focus switching characteristics of our microlens array with several applied voltages. No external voltage was applied in (a), and 5V, 6V, 10V was applied in (b), (c), (d), respectively. Note that the input beam polarization is parallel to the rubbing direction of LC aligning material at the top substrate.

The measured static focal length was 11.4±0.5mm. In a simple model [17], the focal length of microlens, f, is simply given by R / ($n_{e\_LCP} - n_{polymer}$), where n_{e_LCP} is the extraordinary refractive index of the LCP and R is the radius of curvature of the surface relief structure. Assume that the incident polarization emerging at LCP layer is parallel to the LCP alignment direction. From the measured surface profile we can derive the curvature (R) of used our microlens array structure, R = 1252μm, and the resultant theoretical value of the focal length is calculated to be 10.1mm. This is almost matched to the experimentally measured result.

4.4 Focused Beam Profile Variation of Device

In final, the beam profile variations as changing applied voltages were examined as shown in the Fig. 7. The focused beam intensity was diminished gradually as increasing an applied voltage. In Fig. 7, the focused intensity was decreased almost 30% at the application of 5V and finally disappeared with 10V application. These results were well corresponded with the photographic evidence of Fig. 6. The FWHM (Full Width at Half Maximum) at 0V was about 18μm.

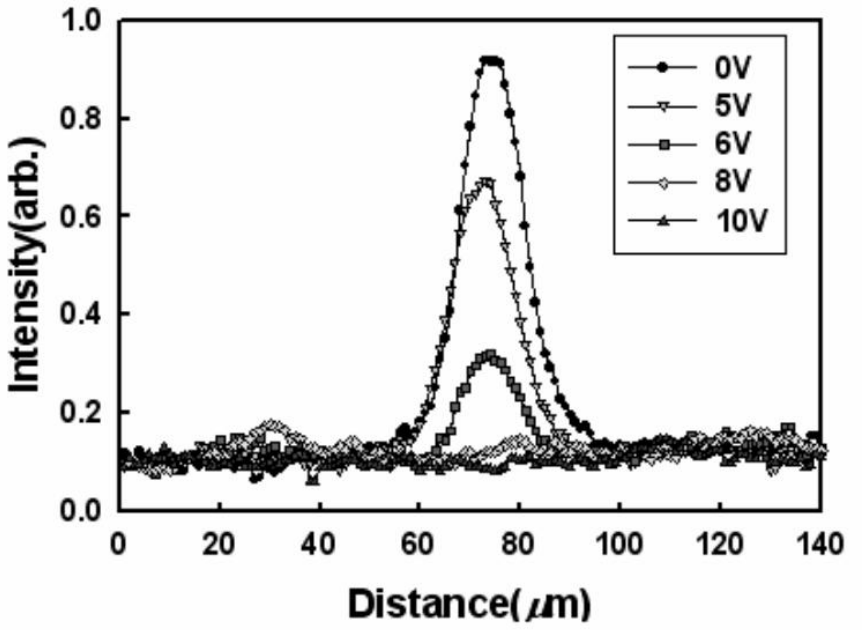

Fig. 7. The intensity profile variations of focusing spot at the focal plane. The intensity of focused spot was represented by arbitrary unit and FWHM of 0V application was about 18μm.

5. CONCLUSION

We have demonstrated the dynamic focusing microlens array by using a LCP, a UV curable photopolymer and nematic LC. The sandwiched system of UV polymer concave relief structure and complementary birefringent LCP layer provides the focusing role of input beam depending on the incident polarization state at the LCP interface. For control of LC microlens focusing characteristic, TN LC structure was added as electro-optical modulation layer. The fine focusing and switching property of device were experimentally examined by a focused image monitoring and focusing spot intensity analysis. Due to the separate operation of polarization controlling and beam focusing at twisted LC layer and polymer microlens layer, suggested LC microlens shows stable and enhanced dynamic focusing characteristics of device. Moreover, by using LCP as focusing layer with flat boundary, we can eliminate the LC's nonlinear GRIN effect for driving range as well as obtain a simple fabrication from LC molecular aligning ability of LCP. In conclusion, this dynamic LC microlens array is expected to be highly applicable for switching device, beam modulator in diverse systems like optical communication and 3-D imaging.

ACKNOWLEDGEMENT

This work was supported in part by Samsung Electronics co. Ltd. and the Korea Research Foundation Grant funded by the Korean Government (MOEHRD) (KRF-2005- 005-D00165).

REFERENCES

1. Y. Choi, J.-H. Park, J.-H. Kim and S.-D. Lee, "Fabrication of a focal length variable microlens array based on a nematic liquid crystal," *Opt. Mater.* 21, 643-646 (2002).
2. Y. Choi, C.-J. Yu, J.-H. Kim and S.-D. Lee, "Fast switching characteristics of surface-relief microlens array based on a ferroelectric liquid crystal," *Ferroelectrics* 312, 25-30 (2004).

3. Y. Choi, Y.-T. Kim, J.-H. Kim and S.-D. Lee, "Polarization independent static microlens array in the homeotropic liquid crystal configuration," *Mol. Cryst. Liq. Cryst.* 433, 191-197 (2005).
4. A. F. Naumov, G. Love, M. Yu. Loktev and F. L. Vladimirov, "Control optimization of spherical modal liquid crystal lenses," *Opt. Express* 4(9), 344-352 (1999).
5. M. Ye, Y. Yokoyama and S. Sato, "Liquid crystal lens with voltage and azimuth-dependent focus," *Proc. of SPIE* 5639, 124-128 (2004).
6. H.-S. Ji, J.-H. Kim and S. Kumar, "Electrically controllable microlens array fabricated by anisotropic phase separation from liquid-crystal and polymer composite materials," *Opt. Lett.* 28(13), 1147-1149 (2003).
7. J.-H. Kim and S. Kumar, "Fast switchable and bistable microlens array using ferroelectric liquid crystals," *Jpn. J. Appl. Phys.* 43(10), 7050-7053 (2004).
8. J.-H. Kim and S. Kumar, "Fabrication of electrically controllable microlens array using liquid crystals," *J. of Lightw. Technol.* 23(2), 628- (2005).
9. D.-W. Kim, C.-J. Yu, H.-R. Kim, S.-J. Kim and S.-D. Lee, "Polarization-insensitive liquid crystal Fresnel lens of dynamic focusing in an orthogonal binary configuration," *Appl. Phys. Lett.* 88, 203505 (2006).
10. H. Ren, Y.-H. Fan and S.-T. Wu, "Polarization-independent phase modulation using a polymer-dispersed liquid crystal," *Appl. Phys. Lett.* 86, 141110 (2005).
11. L. G. Commander, S. E. Day and D. R. Selviah, "Variable focal length microlenses," *Opt. Comm.* 177, 157-170 (2000).
12. B. Wang, M. Ye and S. Sato, "Lens of electrically controllable focal length made by a glass lens and liquid-crystal layers," *Appl. Opt.* 43(17), 3420-3425 (2004).
13. V. Presnyakov and T. Glastian, "Polymer-stabilized liquid crystal lens for electro-optical zoom," *Proc. of SPIE.* 5577, 861-869 (2004).
14. X. Zhang, M. Lokev and G. Vdovin, "Modal liquid crystal lens driven by low voltage produced from a wireless controlling and driving system," *Rev. Sci. Inst.* 76, 043109 (2005).
15. S. Piazolla, and B. K. Jenkins, "Dynamics during holographic exposure in photopolymers for single and multiplexed gratings," *J. of Mod. Opt.* 46(15), 2079-2110 (1999).
16. T. Qian, J.-H. Kim, S. Kumar and P. L. Taylor, "Phase-separated composite films: Experiment and theory," *Phys. Rev. E.* 61(4), 4007-4010 (2000).
17. B. E. A. Saleh and M. C. Teich, *Fundamentals of Photonics*, John Wiley & Sons, New York, 1991.